Computing cross-sections of the workspace of a cable-driven parallel robot with 6 sagging cables having limited lengths

J-P. Merlet

HEPHAISTOS project, Université Côte d'Azur, Inria, France
Jean-Pierre.Merlet@inria.fr

Abstract. Although workspace is essential for the design and control of cable-driven parallel robots very few works have been devoted to this topic when sagging cables are considered, most probably because of the complexity of the cable model. In this paper we consider a CDPR with 6 sagging cables whose lengths have a limited maximal value. We propose an algorithm to compute the border of horizontal cross-section of the workspace for a given altitude and orientation of the platform. We show that the singularity of the inverse kinematics equations have to be taken into account for a proper determination of the border.

Keywords: cable-driven parallel robots, saggging cables, workspace

1 Introduction

Workspace is an essential element for the design and control of a robot. As far as parallel robots with rigid legs are concerned efficient algorithms have been proposed to compute the border of cross-section of the workspace when the orientation and altitude are fixed, taking into account various limitations such as constraints on the leg lengths, on the amplitude of the passive joint motion or interference between the legs [6]. For cable-driven parallel robots (CDPR) the calculation is somewhat more complex because the signs of the cable tensions have to be taken account. For CDPR having *ideal* cables (no deformation due to the weight of the cable, no elasticity) a cable will have to be taken into account only if its tension is positive. Workspace calculation is therefore no more only a geometrical problem but a kineto-static problem. Several papers have addressed workspace calculation of 6 d.o.f. CDPR with ideal cables but considering only tension limitation [1–3],[4, 5], [7],[9, 11], [17, 18],[21–23] while CDPR with elastic cables have been less addressed [10, 13]. The workspace of planar robot with sagging cables has been presented in [19] while, to the best knowledge of the author, 6 d.o.f CDPR has been considered only in [12]. However this paper has only considered as constraint the singularity of the inverse kinematic equations (IK). Our motivation for this work is to introduce another constraint, namely an upper limit on the cable lengths, although we will see that the singularity of the IK has to be taken into account. In this paper we will consider CDPRs with only six cables, this limitation being explained in the next section.

2 Inverse and forward kinematics

In this paper we will use the Irvine sagging cable model that is valid for elastic and deformable cable with mass [8] and that has been shown to be in very good agreement with experimental result s[20]. This model is established in the cable plane in which we have $A_i = (0, 0)$ as upper attachment point of the cable and $B_i = (x_b \geq 0, z_b < 0)$ as lower attachment point. Vertical and horizontal forces $F_z, F_x > 0$ are exerted on the cable at point B_i. For a cable with length at rest L_0 the coordinates of B are given by [8]:

$$x_b = F_x(\frac{L_0}{EA_0} + \frac{sinh^{-1}(F_z) - sinh^{-1}(F_z - \frac{\mu g L_0}{F_x})}{\mu g}) \tag{1}$$
$$z_b = \frac{F_z}{EA_0} - \mu g L_0^2/2 + \frac{\sqrt{F_x^2 + F_z^2} - \sqrt{F_x^2 + (F_z - \mu g L_0)^2}}{\mu g}$$

where E is the Young modulus, A_0 the cable cross-section area, L_0 the cable length at rest and μ the cable linear density. We consider a CDPR with $n \geq 6$ cables which is suspended i.e. the winches output point A_i is always higher than the attachment point B_i of the cable on the platform. If the pose of the platform is given, then the IK unknowns are the $3n$ (F_x^i, F_z^i, L_0^i). We consider the vector $\mathbf{A_iB_i}$ with components x_r^i, y_r^i, z_r^i and define the angle α_i such that

$$x_r^i \sin(\alpha_i) + y_r^i \cos(\alpha_i) = 0 \tag{2}$$

If $(F_x^i, 0, F_z^i)$ are the components of the force that is applied by the platform on the cable in its plane, then the force exerted by the cable on the platform at B_i may be written in the reference frame as $\mathbf{F_a^i} = (-F_x^i \cos(\alpha_i), -F_x^i \sin(\alpha_i), -F_z^i)$. We assume that the platform is submitted only to gravity which exert a vertical force $\mathcal{F}$ and no torque around the platform center of mass C. Hence the mechanical equilibrium imposes

$$\sum_{j=1}^{j=n} \mathbf{F_a^j} + \mathcal{F} = \mathbf{0} \qquad \sum_{j=1}^{j=n} \mathbf{CB_i} \times \mathbf{F_a^j} = \mathbf{0} \tag{3}$$

With these 6 constraints and the $2n$ provided by (1) we have $2n + 6$ constraints for $3n$ unknowns. If $n = 6$ we have a square system that will admit in general a finite number of solution(s) while if $n > 6$ there may be an infinite number of solutions. In this paper we will assume that $n = 6$ to deal with a finite number of solution(s). Note that it has been shown that solving the IK for $n = 6$ is a difficult task and may have indeed several solutions [15, 14].

For the forward kinematics problem (FK) the length L_0^i are known and the pose of the platform has to be determined. The unknowns are the 6 parameters $\mathbf{X}$ defining the pose of the platform and the $2n$ (F_x^i, F_z^i) for a total of $2n + 6$ unknowns. As for the constraints we have the $2n$ constraints (1) and the 6 constraints of the mechanical equilibrium (3). Note that it is useful to add the $n\alpha_i$ as unknowns and the n equations (2) as constraints so that we have $3n +$

6 unknowns/constraints. Therefore the forward kinematics is always a square system that is very difficult to solve and admit usually several solutions. It is important to note that both the FK and IK are **not algebraic** as they involve inverse hyperbolic functions.

3 Workspace

We are interested in calculating cross-sections of the workspace of a CDPR with 6 cables for given altitude and orientation of the platform under the constraint that the cable lengths L_0 cannot exceed a limit L_0^m. The position of C will be denoted x, y, z. If we let x, y be free the FK has 26 unknowns and 24 equations which therefore describe a surface. If we set one of the L_0 to L_0^m the FK will describe a 1-dimensional variety, i.e. a curve in the $x-y$ plane that will be the border of the workspace. Unfortunately being given the FK equations the elimination of F_x^i, F_z^i, α_i from the FK in order to get an implicit equation $G_i(x, y) = 0$ seems to be very difficult. We will thus use another approach: basically we will determine poses potentially on the border and we will use a continuation approach to obtain a polygonal approximation of the G_i curve. Hence the first step of the algorithm is to find poses that may be on the border, that will be denoted *extremal poses*.

3.1 Finding possible extremal poses

An extremal poses is characterized by the property that at least one of its IK solution has at least one L_0 being equal to L_0^m. For finding such pose we will consider a pose $\mathbf{X_0}$, called an *initial pose*,that is most probably inside the workspace and compute its n IK solution(s) using the method proposed in [14]. We consider the pose $\mathbf{X_1}$ defined by the coordinates $(x_0 + \epsilon, y_0)$ where ϵ is a small value that is determined with the Kantorovitch theorem so that the IK system is guaranteed to have a single solution around $\mathbf{X_0}$ which is obtained by using the Newton-Raphson scheme using as initial guess the solution obtained for $\mathbf{X_0}$. We then check if for $\mathbf{X_1}$ all the L_0^j satisfies $L_0^j \leq L_0^m$. If one of the the L_0^j is close to L_0^m we consider the FK equations with x as unknown and impose $y = y_0, L_0^j = L_0^m$. Solving this system with Newton provides an extremal point for one of the branch of the IK at $\mathbf{X_0}$. This extremal point lies on a potential arc for the border (that will be denoted S_j^k), that is associated to $L_0^j = L_0^m$, where k denotes the solution number of the IK at $\mathbf{X_0}$ that has been used to derive $\mathbf{X_1}$. If the L_0 at $\mathbf{X_1}$ all satisfies $L_0^j \leq L_0^m$, then we repeat a motion along the $x+$ direction to find a new pose $\mathbf{X_2}$ and so on until we find an extremal pose.

This process may be repeated by moving from $\mathbf{X_0}$ in the $x-, y+, y-$ directions. After this step we have a set of extremal poses $\mathbf{X_j^e}, \mathbf{X_k^e}, \ldots$ that belong to different arcs $S_j, S_k, \ldots$. We may now present the continuation algorithm that allow us to obtain a polygonal approximation of the arcs $S_j, S_k, \ldots$.

3.2 The continuation algorithm

Let $\mathbf{X_l} = (x_l, y_l)$ be an extremal pose, that has been obtained when moving along the $x+$ direction, lying on the curve S_l, and such that $L_0^l \approx L_0^m$. We then consider a pose $\mathbf{X_k}$ whose y coordinate will be set to $y_l - \gamma$, where $\gamma > 0$ is very small. We set L_0^l to L_0^m and by using Newton we are able to determine the x coordinate of $\mathbf{X_k}$ so that this pose belongs to S_l. With $\mathbf{X_l}, \mathbf{X_k}$ on S_l we are able to get an approximation of the unit tangent vector $\mathbf{T_l^k}$ of S_l at $\mathbf{X_k}$. We consider the largest component u of $\mathbf{T_l^k}$ and define $x(y)_{k+1} = x(y)_k + \epsilon u$. The value of ϵ is determined using Kantorovitch theorem so that Newton is able to calculate $y(x)_{k+1}$ such that $\mathbf{X_{k+1}} = (x_{k+1}, y_{k+1})$ belongs to S_l. We check if $\mathbf{X_{k+1}}$ is such that $L_0^j \leq L_0^m$ for all $j \in [1,6], j \neq l$. If this is the case we have obtained a new pose on S_l and we repeat the process. The continuation process stops in the following cases:

- if L_0^j, $j \neq l$ is close to L_0^m we consider the IK with $L_0^l = L_0^m$ and $L_0^j = L_0^m$ with free x, y and use Newton with $\mathbf{X_k}$ as solution guess to solve this system. At this pose we have obtained a special extremal pose, called an *end-point* of S_l, which has the property of having 2 cable lengths equal to L_0^m
- we get a pose $\mathbf{X_u}$ that is very close to a previously determined $\mathbf{X_v}$ on S_l. This means that S_l is a closed loop

When the continuation has stopped we will start a new continuation process for S_l using $-\mathbf{T_l^k}$ for fixing the continuation direction. This continuation process is repeated for all starting points of all branches.

3.3 Finding new starting points

When the continuation has completed we consider the set of end-points that has been obtained. Each of the end-point $\mathbf{X_l^e} = (x_l^e, y_l^e)$ originates from an arc S_l that meets another arc S_k. We examine if any arc S_k that has been previously determined includes $\mathbf{X_l^e}$. If this not the case we consider the 4 IK problem with $x = x_l^e + \pm\epsilon$ or $y = y_l^e \pm \epsilon$, $x(y)$ being free and L_0^k set to L_0^m. For each of this IK we use Newton with as initial guess the F_x, F_z, L_0 obtained at $\mathbf{X_l^e}$ and $x_l^e(y_l^e)$ as guess for the unknown $x(y)$ As soon as we get one solution that satisfy $L_0^u \leq L_0^m$ for all u in [1,6], $u \neq k$, then we have obtained a new starting point for the branch S_k and we use the continuation algorithm to determine the arc S_k. This process is repeated until all end-points belongs to one of the determined S_l. This normally ensure that we have determined a closed-region that will represent the external border of the workspace. Our algorithm provides a polygonal approximation of the border whose vertices are guaranteed to belong to the border. A question arise however: between two successive vertices the border is assumed to be close to the segment joining the 2 vertices but may the real border be significantly different from the segment ? The answer to this question is no as the Kantorovitch theorem is based on the evaluation of the maximum of the norm of the Hessian matrix all over a ball centered at one vertex that enclose the next vertex and a drastic change of the border will be reflected on the maximum of the norm.

3.4 Example

We consider as example our large scale robot MARIONET-CRANE [16], probably one of the largest CDPR ever deployed. This robot is a suspended CDPR with 6 cables, whose A_i, B_i coordinates are given in table 1. We set $L_0^m = 25m$

x	y	z	x	y	z
-325.9	-47.5	882.6	942.1	-348.2	1155.5
953.8	379.7	1153.3	557.0	2041.4	870.4
-250.5	1681.0	864.9	-334.2	942.1	878.8

x	y	z	x	y	z
-10	-93	-3	10	-93	-3
27	50	-7	27	50	-7
-27	50	-7	-27	50	-7

Table 1. Coordinates of the A_i, B_i points on the base and on the platform (in cm)

and use $x = 2, y = 8$ as initial point for finding starting points. At this point the IK has a single solution and we use the method described in section 3.1 for finding extremal points on S_5, S_6. These points are used to compute these arcs (figure 1) with the continuation algorithm of section 3.2. Using the end-points of these arcs we find new starting points for S_3, S_4 by using the strategy described in section 3.3 and the continuation algorithm allows us to establish these arcs. At this stage there is no new starting point and we get the workspace presented in figure 1. Although it seems that the workspace is a closed-region, details of

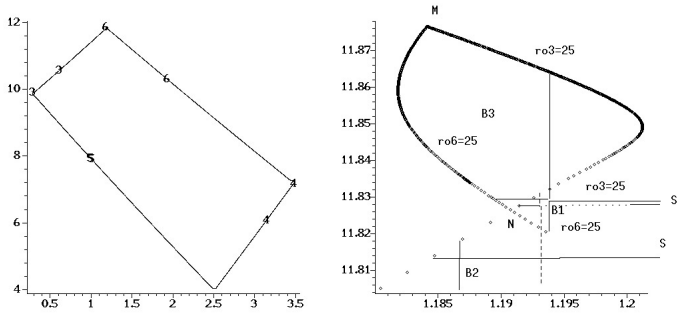

Fig. 1. The workspace border for $L_0^m = 25m$ and a detail of its upper-left corner

the upper-left corner of the workspace (presented in figure 1) show that the curves S_3, S_6 intersect at two poses M, N. The pose M is an end-point of theses curves but the point N is not. Indeed the IK at N has 2 solutions: one with $L_0^3 = L_0^m, L_0^6 < L_0^m$ and another one with $L_0^6 = L_0^m, L_0^3 < L_0^m$. Let us consider the pose $B2$ that is very close of S_3 so that Newton can be used for finding one IK solution for B_2. Starting from B_2 if we move along the $x-$ or $y+$ direction

we end up at a pose on S_3 while moving along the $y-$ direction we end up on S_5. But if we move along $x+$ we cross S_6 and end up in a singular configuration. Now consider $B1$ that is close to S_3 but outside the determined workspace. This pose has 2 valid IK solutions which shows that we have missed reachable poses. For one of them we reach S_3 if we move along the $x-, y+$ direction, S_5 for $y-$ and a singularity for $x+$. For the other one when moving along $x-$ we cross S_3 and stop at S_6 while when moving along $y-$ we stop at S_6. When moving along $x+$ we reach a singularity while when moving along $y+$ we cross S_3 once and end up on another part of S_3.

From this analysis it appears first that we have to perform a local analysis if two S_j and S_k curves intersect but not at an end-point. Finding such an intersection point is not difficult as the polygonal approximation provides an estimate of its x, y coordinates. Then we consider two IK systems, one having $L_0^j = L_0^m$, the other one having $L_0^k = L_0^m$. This amounts to 42 equations in 42 unknowns with a very good initial guess for all them so that Newton will provide the solution. Second the analysis shows that we have to consider singularities that may contribute to part of the border of the workspace.

3.5 Managing singularities

Let us assume that we have found a pose $\mathbf{X_s}$ that has an IK solution but is very close to an IK singularities so that when moving from $\mathbf{X_s}$ in a given direction $\mathbf{v}$ we are no more able to use Newton as the IK become singular at $\mathbf{X_s^1} = \mathbf{X_s} + \epsilon\mathbf{v}$. A continuation scheme may be designed to follow the singularity curve. First we use Newton to determine an IK solution for a pose $\mathbf{X'_s}$ that is close to $\mathbf{X_s}$ but not on the line that includes $\mathbf{X_s}$ with direction $\mathbf{v}$. From $\mathbf{X'_s}$ we move along $\mathbf{v}$ until we reach a pose $\mathbf{X_s^2}$ that is singular. An approximation of the tangent unit vector $\mathbf{T_s}$ of the singularity curve may then be obtained from $\mathbf{X_s^1}, \mathbf{X_s^2}$. Let $\mathbf{N_s}$ be an unit vector that is perpendicular to $\mathbf{T_s}$ and such that $\mathbf{X_s X_s^1}.\mathbf{N_s} < 0$. We consider then a new pose $\mathbf{X_3} = \mathbf{X'_s} + \gamma\mathbf{T_s} + \delta\mathbf{N_s}$ where γ has a small value and δ is a small positive constant. This pose is designed so that $\mathbf{X_3}$ lies on the same side of the line $\mathbf{X_s^1 X_s^2}$ than $\mathbf{X_s}, \mathbf{X'_s}$ and sufficiently away from the singularity curve so that we can compute its IK solution by using Newton with the solution at $\mathbf{X'_s}$ as initial guess. From $\mathbf{X_3}$ we then moves in the direction $-\mathbf{N_s}$ by small increment until we reach a singular pose $\mathbf{X_s^3}$. This process is repeated until we reach a pose $\mathbf{X_s^n}$ that is very close to a S_j curve and is repeated by starting from $\mathbf{X_s}$ but using $-\mathbf{T_s}$ as motion direction.

This strategy has been used in our example using the singular pose that has been found by moving from $B1$ in the $x+$ direction. We find a singularity curve that is displayed in figure 2. The analysis of this new region shows that in the region `U2NU1U3` the IK has two solutions meaning that any motion in this zone may be executed by following two different kinematic branches. For one of this branch the motion is restricted to lie in the region `U0NU1U3` while for the other branch it is restricted to `U2NMU1U3`. Any pose in the region `NMU1` is reachable but a specific motion strategy may have to be designed. For example if the CDPR has to move from $B2$ to $B3$ it will have first to move in the region `U0NU1U3` e.g.

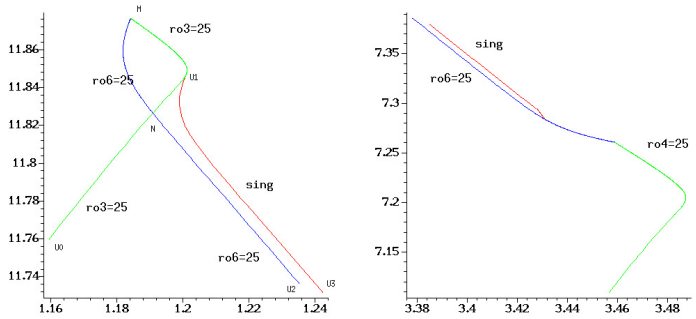

Fig. 2. View of the singularity curve close to N (left) and its connection to S_6 (right)

to $B1$) by following the same kinematic branch than at $B2$. Then at $B1$ the cables lengths will have to be adjusted to get to the other available kinematic branch and then the CDPR may move toward $B3$.

The workspace calculation has been implemented in Maple but a rough approximation of the computation time for an algorithm implemented in C is about 5 minutes for computing a cross-section border if no singularity is encountered and about 10mn if there are singularities.

4 Conclusion

Calculating workspace for CDPR with sagging cables is a difficult task because of the complexity of the cable model and because it induces several solutions to the IK. The algorithm proposed in this paper allows one to calculate the workspace border in a reasonable amount of time. Still there are numerous issues that have to be addressed. First of all the algorithm is able to compute the external border of the workspace but may miss void in the inside of the workspace. Second as the computation time is still relatively high one may wonder if it will not be more efficient to start from the workspace border obtained for ideal cable (that is easy and very fast to determine) and use a continuation method on the Young modulus and linear density to slowly modify the shape of the border for getting the result. Finally the case of CDPR with more than 6 cables has to be investigated: the method is available and will be presented in another paper.

References

1. Albus, J., Bostelman, R., Dagalakis, N.: The NIST ROBOCRANE. J. of Robotic Systems **10**(5), 709–724 (July 1993)
2. Aref, M., Taghirad, H.: Geometrical workspace analysis of a cable-driven redundant parallel manipulator: KNTU CDRPM. In: IEEE Int. Conf. on Intelligent Robots and Systems (IROS), pp. 1958–1963. Nice, France (September, 22-26, 2008)

3. Diao, X., Ma, O.: Workspace determination of general 6 d.o.f. cable manipulators. Advanced Robotics **22**(2-3), 261–278 (2008)
4. Duan, Q., Duan, X.: Workspace calculation and quantification calculations of cable-driven parallel robots. Advances in Mechanical Engineering **2014** (2014)
5. Ferraresi, C., Paoloni, M., F., P.: A new methodology for the determination of the workspace of six-dof redundant parallel structures actuated by nine wires. Robotica **25**(1), 113–120 (January 2007)
6. Gosselin, C.: Determination of the workspace of 6-dof parallel manipulators. ASME J. of Mechanical Design **112**(3), 331–336 (September 1990)
7. Gouttefarde, M., Daney, D., Merlet, J.P.: Interval-analysis based determination of the wrench-feasible workspace of parallel cable-driven robots. IEEE Trans. on Robotics **27**(1), 1–13 (February 2011).
8. Irvine, H.M.: Cable Structures. MIT Press (1981)
9. Jeong, J., Kim, S., Kwak, Y.: Kinematics and workspace analysis of a parallel wire mechanism for measuring a robot pose. Mechanism and Machine Theory **34**(6), 825–841 (August 1999)
10. Korayem, M., Bamdad, M., Saadat, M.: Workspace analysis of cable-suspended robots with elastic cable. In: IEEE International Conference on Robotics and Biomimetics, 2007. ROBIO 2007, pp. 1942–1947 (2007)
11. Lim, W., et al.: A generic force closure algorithm for cable-driven parallel manipulators. Mechanism and Machine Theory **46**(9), 1265–1275 (September 2011)
12. Merlet, J.P.: Computing cross-sections of the workspace of cable-driven parallel robots with 6 sagging cables. In: Computational Kinematics. Poitiers (2017)
13. Merlet, J.P.: On the workspace of suspended cable-driven parallel robots. In: IEEE Int. Conf. on Robotics and Automation. Stockholm (May, 16-20, 2016)
14. Merlet, J.P.: A new generic approach for the inverse kinematics of cable-driven parallel robot with 6 deformable cables. In: ARK. Grasse (June, 27-30, 2016)
15. Merlet, J.P.: On the inverse kinematics of cable-driven parallel robots with up to 6 sagging cables. In: IEEE Int. Conf. on Intelligent Robots and Systems (IROS), pp. 4536–4361. Hamburg, Germany (September 28- October 2, 2015)
16. Merlet, J.P., Daney, D.: A portable, modular parallel wire crane for rescue operations. In: IEEE Int. Conf. on Robotics and Automation, pp. 2834–2839. Anchorage (May, 3-8, 2010).
17. Ouyang, B., Shang, W.W.: A new computation method for the force-closure workspace of cable-driven parallel manipulators. Robotica **33**(3), 537–547 (March 2015)
18. Pusey, J., et al.: Design and workspace analysis of a 6-6 cable-suspended parallel robot. Mechanism and Machine Theory **139**(7), 761–778 (July 2004)
19. Riehl, N., et al.: On the static workspace of large dimension cable-suspended robots with non negligible cable mass. In: 34th Annual Mechanisms and Robotics Conference. Montréal (August, 15-18, 2010)
20. Riehl, N., et al.: On the determination of cable characteristics for large dimension cable-driven parallel mechanisms. In: IEEE Int. Conf. on Robotics and Automation, pp. 4709–4714. Anchorage (May, 3-8, 2010)
21. Stump, E., Kumar, V.: Workspaces of cable-actuated parallel manipulators. ASME J. of Mechanical Design **128**(1), 159–167 (January 2006)
22. Tavolieri, C., Ceccarelli, M., Merlet, J.P.: A workspace analysis of a fully constrained cable-based parallel manipulator by using interval analysis. In: Musme. San Juan, Argentina (April, 8-12, 2008)
23. Verhoeven, R.: Analysis of the workspace of tendon-based Stewart platforms. Ph.D. thesis, University of Duisburg-Essen, Duisburg (2004)